Aalto University

Aaltodoc

OPEN ACCESS

Author(s): Wu, Fan & Tsuneta, Taku & Tarkiainen, Reeta & Gunnarsson, David & Wang, Tai-Hong & Hakonen, Pertti J.

Title: Shot noise of a multiwalled carbon nanotube field effect transistor

Year: 2007

Version: Final published version

Please cite the original version:

Shot noise of a multiwalled carbon nanotube field effect transistor

Fan Wu,[1] Taku Tsuneta,[1] Reeta Tarkiainen,[1] David Gunnarsson,[1] Tai-Hong Wang,[2] and Pertti J. Hakonen[1]

[1]*Low Temperature Laboratory, Helsinki University of Technology, P.O. Box 2200, FIN-02015 HUT, Finland*
[2]*Institute of Physics, Chinese Academy of Sciences, 100080, Beijing, China*
(Received 2 August 2006; revised manuscript received 4 January 2007; published 21 March 2007)

We have investigated shot noise in a 6-nm-diameter, semiconducting multiwalled carbon nanotube field effect transistor at 4.2 K over the frequency range of $600-950$ MHz. We find a transconductance of $3-3.5$ μS for optimal positive and negative source-drain voltages V. For the gate referred input voltage noise, we obtain 0.2 and 0.3 μV$/\sqrt{\text{Hz}}$ for $V>0$ and $V<0$, respectively. As effective charge noise, this corresponds to $(2-3) \times 10^{-5}$ $e/\sqrt{\text{Hz}}$.

Semiconducting single-walled carbon nanotubes have been shown to provide extraordinary field effect transistors[1,2] (FETs) in which the modulation of Schottky barriers is often an important factor.[3,4] Intrinsic performance limits of these devices due to the mobility of charge carriers have been investigated recently.[5–10] Transconductances up to $g_m = \frac{\Delta I_{ds}}{\Delta V_g} = 8700$ μS$/\mu$m, relating the change in drain-source current I_{ds} to gate voltage V_g, have been reported in single-walled carbon nanotubes (SWNTs) on top of a high-κ material (SrTiO$_3$).[12] It has been shown experimentally that g_m increases as ϕ^2 with the tube diameter ϕ.[10] This, however, takes place at the expense of a reduced energy gap, which sets an upper limit for the diameter of room-temperature devices.

Another important issue for typical FET applications is the noise power generated by the device. Here, we are interested in the uncoupled shot noise performance and neglect the nonequilibrium $1/f$ noise,[11] the understanding of which is a prerequisite for the proper noise minimization with a finite source impedance. In general, the low-frequency current noise $S(\omega) = \int e^{i\omega t} \langle \delta i(t) \delta i(0) \rangle$ in a mesoscopic sample can be written as

$$S = \frac{4 k_B T}{R}(1-F) + F 2 e I \coth\left(\frac{eV}{2 k_B T}\right), \quad (1)$$

where R is the resistance of the sample, T is the temperature, F denotes the Fano factor, and V is the dc biasing voltage. The Fano factor depends on transmission coefficients of the transport channels of the sample, as well as on inelastic processes causing energy relaxation, which are known to lower the shot noise.[13] The best uncoupled performance corresponds to the minimization of S/g_m^2 which yields the minimum equivalent voltage noise at the input. Here, we present an experimental determination of this noise quantity in a semiconducting nanotube device.

In our 4 K measurement setup, *IV* characteristics and differential conductance properties are measured in a regular two-terminal configuration, supplemented with a radio-frequency noise amplification circuitry. Bias tees are used to separate dc bias and the current-dependent noise signal at radio frequencies. We use a low-noise, cooled amplifier[14] with a working frequency range of $600-950$ MHz for suppressed $1/f$ noise. The total gain of the amplifier chain

amounts to 80 dB (16 dB at 4.2 K) and the noise temperature of the whole setup is roughly 10 K; for detection, we used a zero-bias Schottky diode. A switch and a high-impedance tunnel junction are used to calibrate the gain and the bandwidth; i.e., we can determine the Fano factor of our carbon nanotube (CNT) samples by direct comparison with the noise measured on a tunnel junction sample having $F = 1$.

We determine the Fano factor at drain-source voltage V_{ds} as

$$F = \frac{S(I_{ds}) - S(0)}{2 e I} = \frac{1}{2 e I_{ds}} \int_0^I \left(\frac{dS}{dI_{ds}}\right) dI, \quad (2)$$

where $\left(\frac{dS}{dI_{ds}}\right)$ represents the differentially measured noise using a small modulation voltage of 0.5 mV at 18.5 Hz on top of V_{ds}. At large currents, this determination coincides with the ordinary definition of Fano factor. In the intermediate bias region, there will be corrections that depend on the ratio of differential resistance $\frac{dV_{ds}}{dI_{ds}}$ to V_{ds}/I_{ds} due to thermal noise coupling, but these corrections are negligible for the analysis in this paper.[15,16] Because the sample impedance is not matched to the preamplifier, we are able to measure shot noise only at currents of $I > I_{th}$, where $F I_{th}$ must be around 0.01 μA.

Our tube material, provided by Koshio *et al.*, was grown using plasma-enhanced growth without any metal catalyst.[17] The tubes were dispersed in dichloroethane and, after 15 min of sonication, they were deposited onto thermally oxidized, strongly doped Si wafers. A tube of 4 μm in length was located with respect to alignment markers using a field emission scanning electron microscope (FE-SEM) Zeiss Supra 40. Subsequently, Ti contacts with width of 900 nm were made using standard overlay lithography: 10 nm titanium layer was covered by 70 nm Al in order to facilitate proximity-induced superconductivity at subkelvin temperatures. The length of the tube section between the contacts was 1200 nm. The electrically conducting body of the silicon substrate was employed as a back gate, separated from the sample by 100 nm of SiO$_2$. The sample was bonded to a sample holder with miniature, 6 GHz bias tees using 25 μm Al bond wires with less than 10 nH of inductance.

Differential conductance $G_d = \frac{dI_{ds}}{dV_{ds}}$ for our sample is illus-
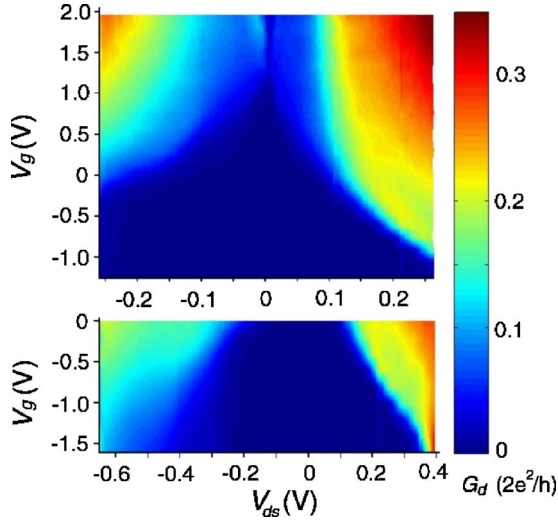
FIG. 1. (Color online) Normalized differential conductance G_d/G_0 with $G_0=2e^2/h$ for our semiconducting sample measured at 4.2 K on the gate V_g vs bias voltage V_{ds} plane: the color scale is given by the bar on the right. Lower figure is measured with larger source-drain voltage at V_g around -1 V. For the sample parameters, see text.

trated in Fig. 1 in units of $G_0=2e^2/h$. G_d is seen to display a roughly linear conductance, on the order of $0.1G_0$, at voltages $V_{ds}=-0.1\cdots+0.1$ V and $V_g=1-4$ V. When current is increased to $I_{ds}=1$ μA, G_d becomes on the order of $0.2G_0$, which is a typical value for metallic plasma-enhanced chemical vapor deposition (PECVD) tubes of the same batch. Thus, there is no obvious difference in conductance between semiconducting and metallic specimens, as observed in SWNT tubes.[18]

Our nanotube sample is clearly *n*-type doped initially.[19] Looking at $G_d(V_{ds},V_g)$, we deduce that the charge neutrality point where E_F corresponds to the intrinsic level in the bulk of the tube is located around $V_g=-1.7$ V, which also corresponds to the maximum gap of 0.8 V. Using the gate capacitance $C_g=18$ aF and total island capacitance of 0.4 fF (see below), we find that the initial shift of the Fermi level from the intrinsic level is approximatively -0.08 V. This differs substantially from the value of $+0.4$ V that has been reported for multiwalled carbon nanotubes (MWNTs).[20] Typically, *n*-type doping in nanotubes (NTs) has been obtained using potassium deposition.[21,22]

The capacitance of our back gate was measured by observing Coulomb modulation in the range $V_g=2,\ldots,4$ V. The measured periodicity of 8.8 mV corresponds to 18 aF. The island capacitance $C_\Sigma=0.4$ fF, including source, drain, and gate capacitances, was estimated using a geometric capacitance of $C=200$ pF/m in series with a quantum capacitance of similar magnitude along the full length of 4 μm. Owing to the local thinning of the 100 nm SiO_2 oxide due to Al wire bonding, we used gate voltages only up to ±4 V in our studies. In addition, we limited our measurements to currents below 5 μA which is on the same order as typical on-state current in SWNT devices.

The model, which we employ to account for our basic findings, has been proposed and discussed in Ref. 23. There,
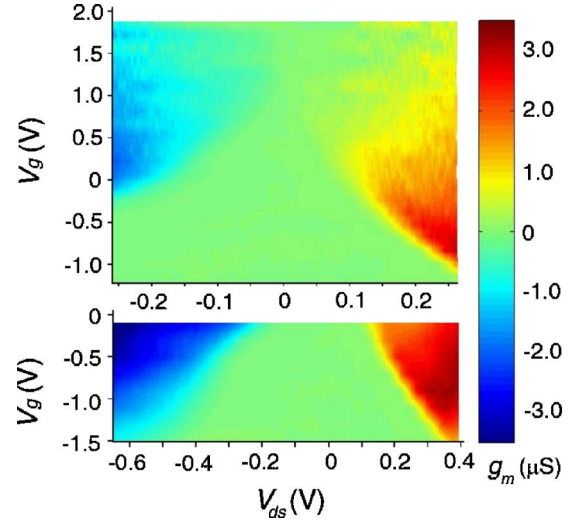

FIG. 2. (Color online) Transconductance g_m as a function of bias V_{ds} and gate voltage V_g. Lower figure is measured with larger source-drain voltage at V_g around -1 V.

it was conjectured that owing to band pinning at the metal-nanotube interfaces, small quantum dots are formed at the ends of the nanotube when the tube is brought into strong inversion by the gate voltage. In our case, this is corroborated by the appearance of another (quasiperiodic) gate modulation in the range $V_g=-0.6,\ldots,-4$ V. This gate period changed from $\Delta V_g=0.13$ V at $V_g\sim-1$ V to $\Delta V_g=0.18$ V at $V_g\sim-2.5$ V. The size of the period is in accordance with the findings in Ref. 23, while the increase in ΔV_g in our data reflects a decrease in the dot size as V_g becomes more strongly negative.

The expected gap for a semiconducting tube of diameter $\phi=6$ nm is approximately $V_{gap}=0.14$ V.[24] If the extra width of the gap were due to the quantum dots at the ends of the tube, their capacitance would be about 1 aF, i.e., <10 nm in length. Room-temperature measurements indicate that the gap indeed is composed of a few smaller components, but we cannot exclude the possibility that, at some large gap value, the tube is broken into more than three quantum dots.

In CNT-FETs, the signature of depletion mode in I_{ds} vs V_g sweeps is the appearance of a threshold voltage, related to current by the form $I_{ds}^2\propto V_g-V_{th}$.[12] Using this form, we obtain $V_{th}=0.25$ V for the pinch-off as an average of positive and negative biasing cases [see Fig. 5(a) below]. When lowering the gate voltage toward V_{th}, the small voltage *IV* curves change from linear to more and more power-law-like: in the range $V_g=1$ V,$\ldots,V_{th}$, the exponent varies from 1 to 3 (in Fig. 1, the exponent of G_d varies from 0 to 2).

Measured transconductance around the pinch-off region is displayed in Fig. 2. The largest magnitude of transconductance is roughly equal at positive and negative biases: ~3 μS at $V>0$ and ~3.5 μS at $V<0$. At positive bias, the optimum is reached in a small region of bias values around $V_{ds}=0.37$ V and $V_g=-0.9$ V, whereas at $V<0$ the maximum value is obtained on a more extended region at $V_{ds}<-0.5$ V around $V_g=0$.

Figure 3(a) illustrates the measured current noise in the range $V_g=-1.2,\ldots,-0$ V which is right below the pinch-off
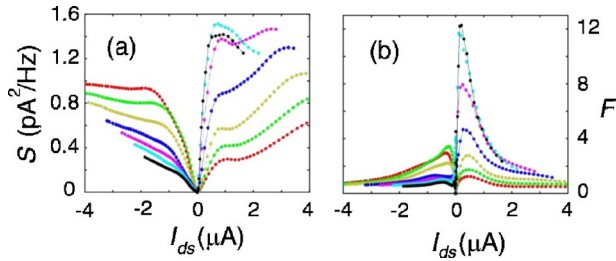
FIG. 3. (Color online) (a) Current noise S integrated over the frequency range of $600-950$ MHz vs current I_{ds} and (b) the corresponding Fano factor. Due to lack of sensitivity, currents below 0.01 μA have been cut off from the plot. The bias voltage varies over $V_{ds}=-1.2,\ldots,0$ V in steps of 0.2 V (from top to bottom at $V_{ds}>0$ and from bottom to top at $V_{ds}<0$)

of threshold V_{th}; the corresponding Fano factor is given in Fig. 3(b). At large negative bias and with large positive bias at $V_g \ll V_{th}$, the noise can be regarded as shot noise from an asymmetric double junction system,[25,26] which yields $F =(\Gamma_1^2+\Gamma_2^2)/(\Gamma_1+\Gamma_2)^2<1$, where Γ_1 and Γ_2 refer to tunneling rates in the two tunnel barriers. At small V_{ds}, especially at $V_{ds}>0$, the measured noise is strongly peaked, and the corresponding Fano factor reaches $F=12$ at its maximum. This behavior may be an indication of noise due to inelastic cotunneling as argued by Onac *et al.* in a SWNT quantum dot at small bias.[27] In our case, however, we believe that a more likely explanation is due to a bias-dependent fluctuator that modulates the transmission at one of the contacts.[28] According to this model, the peak in the noise vs current reflects the movement of the corner frequency of the Lorentzian fluctuation spectrum across the frequency band of the measurement.
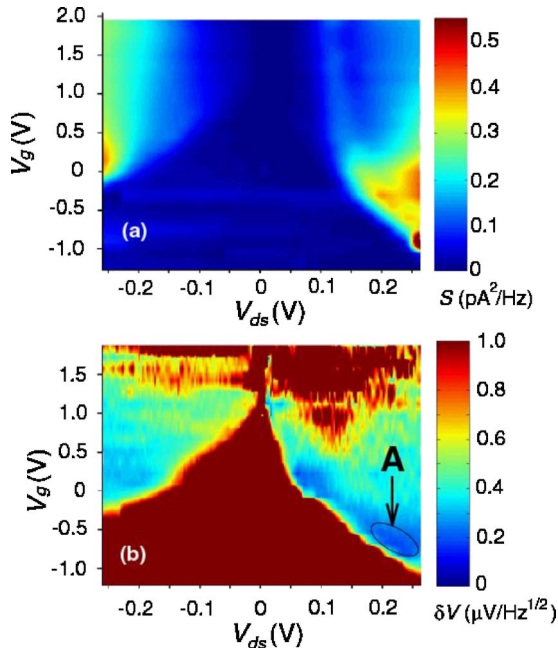

FIG. 4. (Color online) (a) Current noise S over V_g vs V_{ds} plane. (b) Noise power of (a) converted into input voltage noise by dividing by g_m^2. The region of smallest noise has been denoted by an ellipsoid.
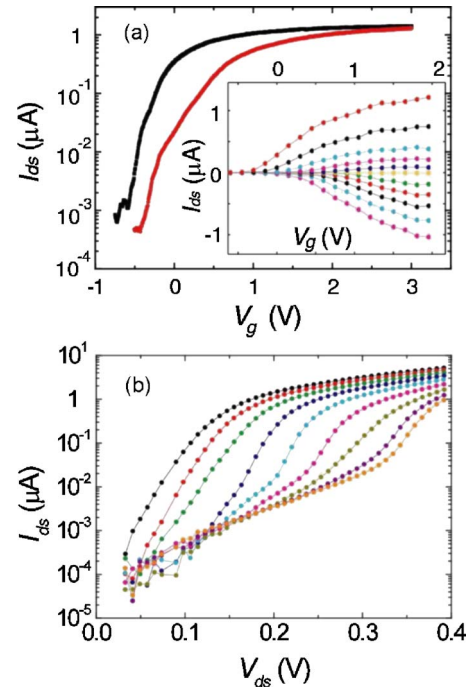

FIG. 5. (Color online) (a) I_{ds} vs V_g at bias voltage $V_{ds}= +0.135$ V ($\square$) and $V_{ds}=-0.135$ V ($\bigcirc$). The inset displays a set of current traces on linear scale measured when at V_{ds} has been stepped from -0.13 to 0.13 V by 26 mV (from bottom to top). (b) I_{ds} vs V_{ds} (>0) curves at $V_g=$const, stepped from -1.6 to 0 V by 0.2 V (from bottom to top).

Initially, the noise increases when the corner frequency approaches the measurement band from below. The decrease at large currents is because the total integrated noise over the Lorentzian spectrum is fixed, and as the corner frequency continues to grow, the noise per unit band has to decrease.[28] Thus, we argue that there are bias-dependent fluctuators in metal-nanotube systems with tunneling rates in the gigahertz regime.

The overall noise characteristics of our device are illustrated in Fig. 4(a). By multiplying S with $1/g_m^2$, we may convert the measured current noise into voltage noise at the gate, which is displayed in Fig. 4(b). Here, we assume that the electrical properties of the tube do not change with frequency up to 800 MHz, as indicated by the experiments by Yu and Burke.[29] The lowest-noise region of operation is marked by A, which is very close to the region of maximum g_m. However, since the variation of g_m is rather slow with V_{ds} and V_g, the optimum noise is located at a local minimum of noise power. Note that, even though negative bias provides larger g_m and smaller Fano factors, the smallest input equivalent voltage noise δV_g is found at $V>0$ because I_{ds} is much smaller at optimum regions at $V>0$ than at $V<0$.

At point A, we find $\delta V_g=0.2$ μV$/\sqrt{\text{Hz}}$. This input voltage noise, in turn, can be converted into charge noise at the gate, which yields $\delta q_g=20$ $\mu e/\sqrt{\text{Hz}}$. At negative bias, our results are about 30% worse, i.e., $\delta q_g=30$ $\mu e/\sqrt{\text{Hz}}$. These values are close to the results obtained in radio-frequency single-electron transistor (rf-SET) setups using impedance matching.[30] Note that no matching circuits have been em-

ployed here and that the noise has been measured over a large band of 600–950 MHz. In a rf-SET setup with hundreds of parallel SETs, a bandwidth of 1 GHz has been achieved, but with a limited charge sensitivity of $\delta q_g = 2$ me/$\sqrt{Hz}$ due to a large input capacitance.[31] Thus, our results suggest that nanotube FETs based on MWNTs may be employed as sensitive charge detectors at high frequencies, rivaling the performance of rf-SETs.

Semiconducting nanotube devices are often described in terms of field effect (FE) mobility corresponding to transconductance $\mu_{FE} = \frac{L}{C_g^*} \frac{\partial G}{\partial V_g} = \frac{L}{C_g^* V_{ds}} \frac{\partial I}{\partial V_g}$, where C_g^* denotes the gate capacitance per unit length.[12] This quantity is employed for the description of the "bulk" properties of the tube when the contribution from the contacts can be neglected. In our case, even though the length of the tube is not extremely large, the resistance of the tube should dominate close to the pinch-off of the device. Gate sweeps at $V_{ds} = \pm 0.135$ V are illustrated in Fig. 5(a). From the figure, we may read at 0.1 μA that conductance I_{ds}/V_{ds} changes by decade/250 mV and by decade/500 mV at positive and negative biases, respectively. This fact that the threshold is sharper at $V_{ds} > 0$ is visible also from the inset of Fig. 5(a) which displays a set of current traces vs V_g measured with stepping V_{ds} over −0.13–0.13 V. The data in Fig. 5 yield for the maximum FE mobility $\mu_{FE} = 1$ m^2/V s, which falls short by a factor of >100 from the value extrapolated for $\phi = 6$ nm using temperature-scaled data of Ref. 10 measured above 50 K for SWNTs with $\phi = 1$–4 nm. This discrepancy indicates that our MWNTs are more strongly diffusive than typical semiconducting SWNTs.

For completeness, Fig. 5(b) displays I_{ds} vs V_{ds} curves of our device when V_g is varied from −1.6 to 0 V in steps of 0.2 V. Using exponential fits $I_{ds} \propto \exp(eV/E_0)$ for currents $I_{ds} < 10$ nA (at $V_{ds} > 0$), we obtain $E_0 = 130$ and 35 mV at $V_g = -1.6$ and −0.4 V, respectively, with a monotonous decrease as a function of V_g. Since the energy scale $E_0 \gg k_B T$ ($T = 4.2$ K), it is likely that the exponential behavior in the small current regime is due to quantum tunneling in Schottky barriers.[32] The applied gate voltage modulates the shape of the barrier, leading to a change in E_0. When 10 nA $< I_{ds} < 100$ nA, E_0 is around 30–40 mV and nearly independent of V_g. Such a change of dependence may signal nonlinear effects in quantum tunneling, or be an indication that the charge transport is governed by two competing (parallel) bottlenecks with different activation energy scales (e.g., tunneling to an innermetallic layer[33]). When V_g is increased above −0.2 V, the I_{ds} vs V_{ds} relation is seen to change gradually from exponential behavior to a power law as the nanotube FET goes from the depletion regime to conducting state.

In summary, we have presented noise investigations on semiconducting nanotube FETs at microwave frequency. We find noise behavior that varies between sub- and super-Poissonian values. The sub-Poissonian values are consistent with double Schottky barrier configuration, while the super-Poissonian results indicate the presence of two-level fluctuators with bias-dependent switching rates exceeding 1 GHz. For the input referred noise, expressed in terms of charge noise on the gate, we find $(2-3) \times 10^{-5}$ e/$\sqrt{Hz}$. Thus, these devices may challenge regular aluminum-based rf-SETs as the ultimate charge detectors.

[1] S. J. Tans, A. R. M. Verschueren, and C. Dekker, Nature (London) **393**, 49 (1998).

[2] A. Javey, J. Guo, Q. Wang, M. Lundstrom, and H. Dai, Nature (London) **424**, 654 (2003).

[3] S. Heinze, J. Tersoff, R. Martel, V. Derycke, J. Appenzeller, and Ph. Avouris, Phys. Rev. Lett. **89**, 106801 (2002).

[4] J. Appenzeller, J. Knoch, V. Derycke, R. Martel, S. Wind, and Ph. Avouris, Phys. Rev. Lett. **89**, 126801 (2002).

[5] A. Javey, J. Guo, M. Paulsson, Q. Wang, D. Mann, M. Lundstrom, and H. Dai, Phys. Rev. Lett. **92**, 106804 (2004).

[6] T. Dürkop, S. A. Getty, E. Cobas, and M. S. Fuhrer, Nano Lett. **4**, 35 (2004).

[7] H. Cazin d'Honincthun, S. Galdin-Retailleau, J. Sée, and P. Dollfus, Appl. Phys. Lett. **87**, 172112 (2005).

[8] Yung-Fu Chen and M. S. Fuhrer, Phys. Rev. Lett. **95**, 236803 (2005).

[9] Z. Chen, J. Appenzeller, J. Knoch, Yu-Ming Lin, and Ph. Avouris, Nano Lett. **5**, 1497 (2005).

[10] X. Zhou, Ji-Yong Park, S. Huang, J. Liu, and P. L. McEuen, Phys. Rev. Lett. **95**, 146805 (2005).

[11] Yu-Ming Lin, J. Appenzeller, J. Knoch, Z. Chen, and Ph. Avouris, Nano Lett. **6**, 930 (2006), and the references therein.

[12] B. M. Kim, T. Brintlinger, E. Cobas, M. S. Fuhrer, Haimei Zheng, Z. Yu, R. Droopad, J. Ramdani, and K. Eisenbeiser, Appl. Phys. Lett. **84**, 1946 (2004).

[13] Ya. M. Blanter and M. Büttiker, Phys. Rep. **336**, 1 (2000).

[14] L. Roschier and P. Hakonen, Cryogenics **44**, 783 (2004).

[15] For details, F. Wu, L. Roschier, T. Tsuneta, M. Paalanen, T. Wang, and P. Hakonen, in *Proceedings of "24th International Conference on Low Temperature Physics: LT24"*, edited by Y. Takano, S. P. Hershfield, S. O. Hill, P. J. Hirschfeld, and A. M. Goldman, AIP Conf. Proc. No. 850 (AIP, Melville, NY, 2006), pp. 1482–1483.

[16] At liquid helium temperature, the crossover between thermal and shot noise takes place at $V_{ds} \sim 1$ mV, which is a small voltage compared with typical V_{ds} values employed in our measurements.

[17] A. Koshio, M. Yudasaka, and S. Iijima, Chem. Phys. Lett. **356**, 595 (2002).

[18] See, e.g., P. L. McEuen, M. Bockrath, D. H. Cobden, Y. G. Yoon, and S. G. Louie, Phys. Rev. Lett. **83**, 5098 (1999).

[19] The issue of doping of carbon nanotubes appears to be an intricate one. As argued by T. Yamada in Appl. Phys. Lett. **80**, 4027 (2002), some of the early experiments can be understood on the

basis of negative doping in NTs even though the common belief is to have positive doping either due to adsorbed oxygen or due to a difference in metal-NT work functions. In our case, we assign the charge neutrality point to the gate value at which the measured conductance is at minimum (averaged over Coulomb effects). This is expected to correspond to $E_F \simeq E_{intrinsic}$ in the bulk of the tube, even though modifications may arise from the quantum dots, located at the ends of the tube (see text) (Ref. 23).

[20] This is with a typical oxygen doping. See M. Kruger, M. R. Buitelaar, T. Nussbaumer, C. Schonenberger, and L. Forro, Appl. Phys. Lett. **78**, 1291 (2001).

[21] M. Bockrath, J. Hone, A. Zettl, P. L. McEuen, A. G. Rinzler, and R. E. Smalley, Phys. Rev. B **61**, R10606 (2000).

[22] J. Appenzeller, J. Knoch, M. Radosavljević, and Ph. Avouris, Phys. Rev. Lett. **92**, 226802 (2004).

[23] J. Park and P. McEuen, Appl. Phys. Lett. **79**, 1363 (2001).

[24] See, e.g., R. Saito, G. Dresselhaus, and M. S. Dresselhaus, Phys. Rev. B **61**, 2981 (2000).

[25] See, e.g., A. N. Korotkov, D. V. Averin, K. K. Likharev, and S. A. Vasenko, in *Single-Electron Tunneling and Mesoscopic Devices*, edited by H. Koch and H. Lübbig (Springer, Berlin, 1992), p. 45.

[26] M. J. M. de Jong and C. W. J. Beenakker, Physica A **230**, 219 (1996).

[27] E. Onac, F. Balestro, B. Trauzettel, C. F. J. Lodewijk, and L. P. Kouwenhoven, Phys. Rev. Lett. **96**, 026803 (2006).

[28] R. Tarkiainen, L. Roschier, M. Ahlskog, M. Paalanen, and P. Hakonen, Physica E (Amsterdam) **28**, 57 (2005). Note that the corner frequency of the fluctuator may go down or up with the bias and the result is qualitatively the same.

[29] Z. Yu and P. J. Burke, Nano Lett. **5**, 1403 (2005).

[30] L. Roschier, P. Hakonen, K. Bladh, P. Delsing, K. W. Lehnert, L. Spietz, and R. J. Schoelkopf, J. Appl. Phys. **95**, 1274 (2004).

[31] S. Gustavsson, D. Gunnarsson, and P. Delsing, Appl. Phys. Lett. **88**, 153505 (2006).

[32] S. N. Levine, *Quantum Physics of Electronics* (Macmillan, New York, 1965), pp. 146–149.

[33] L. Forró and C. Schönenberger, in *Carbon Nanotubes: Synthesis, Structure, Properties and Application*, edited by M. S. Dresselhaus, G. Dresselhaus, and Ph. Avouris (Springer, Berlin, 2001), pp. 329–390.